High deformation effects on the plasticity of ultra-high carbon steel wires

Elena Brandaleze[1]*, Martina Avalos[2] and Mykaylo Romanyuk[1]

[1]*Process Technology: Metallurgy Department, DEYTEMA Center, Universidad Tecnológica Nacional- Facultad Regional San Nicolás, Colón 332, San Nicolás, 2900, Argentina.*

[2]*IFIR-Conicet, Universidad Nacional de Rosario, Ocampo y Esmeralda, Ocampo 210 bis, 2000, Rosario, Argentina*

*Corresponding author

DOI: 10.5185/amp.2018/930
www.vbripress.com/amp

Abstract

Steel wires under severe cold drawing deformation, develop high strength (5-6 GPa) and ductility. For these reasons it is relevant to increase the knowledge on the structural evolution and deformation mechanisms involved during wire drawing process, due to their critical applications such as bridges, cranes and tire cord. This paper presents a comparative study of steel wires (0.84%C) at different deformation stages. The product presents a normal behaviour under torsion test, the mentioned test is normally used to corroborate the wire aptitude. The main objective of the study is to increase the knowledge on the structural evolution after cold drawn considering the deformation mechanisms, cementite dissolution, and epsilon carbide precipitation. The microstructural study was carried out applying light and scanning electron microscopy (SEM-EBSD). The structural information was correlated with results of differential thermal analysis (DTA) and FactSage simulation. The structural study verified the presence of curling phenomenon in the wires. The interlaminar spacing (λ) and the thickness of cementite lamellae in wires cold drawn from 8 mm up to 2 mm of diameter was determined. Finally, the dynamic strain aging, which is promoted by cementite destabilization and the precipitation of epsilon carbide was studied.

Keywords: High carbon steel, cold drawing, epsilon carbide, mechanical properties, texture.

Introduction

In the modern ferrous metallurgy there are great developments about pearlitic wires with high formability, keeping ultra-high mechanical strength [**1, 2**]. Recent articles on ultra-high strength steels reports the phenomenon of cementite dissolution under high percentages of plastic deformation [**3**]. It has been shown that in these steels, the cold drawn process decrease the interlamellar spacing and the thickness of the cementite (Fe_3C) lamellae, due to its dissolution under high deformation [**1, 2, 4**]. The final mechanical properties combination of the pearlitic steel (C≥ 0.84%), allows them to be used in critical applications such as: handing bridge cables, crane cables, tire cord, among others [**5**].

Despite the numerous research done, the understanding of the mechanisms that produce the extraordinary strength of this steels is not fully known yet. The correlation between the properties and microstructure evolution is necessary to understand the mechanisms that promote the ultra-high strength [**6**]. Largely mechanical properties are controlled by different factors: cementite lamellae thickness, lamellae interfaces evolution, texture changes, metallographic texture, crystallographic texture, plastic flow localization, dynamic strain aging and thermodynamic aspect of the cementite dissolution [**1-7**]. The cementite dissolution, produces the over-saturation of the ferrite and also could cause the epsilon carbide precipitation [**2**]. In this paper the microstructure evolution of the pearlitic steel is discussed on wires with different cold drawn deformation levels. A pearlitic steel wire (0.84% C) cold drawn from 8 mm up to 2.2 mm of diameter, are selected. The structure of the samples were studied by optical microscopy, scanning electron microscopy (SEM) and electron backscatter diffraction (EBSD). The interlamellar spacing (λ) and the cementite lamellae thickness of all the samples was measured in the centre and the periphery of the wire. In addition, the ferrite structure evolution with the highest reduction of diameter was studied collecting data by EBSD. The main novelty introduced by this paper is the discussion about the deformation impact of wires cold drawn at different deformation levels. The cementite lamellae refinement and the evolution of the ferrite structure at nano scale is considered. In order to clarify the cementite dissolution process and the iron carbides stabilities in relation with the deformation and temperature, thermal analysis tests

(DTA) were carried out. The peak temperature of the epsilon carbide precipitation was determined in each sample. Furthermore, the stability of iron carbides was evaluated using thermodynamic simulation performed with the software FactSage, considering the chemical composition of the steel and the cold drawn conditions.

Experimental

Materials

Wires of ultra-high carbon content (C 0.84%) deformed under different cold drawing levels were selected. The diameter reductions considered are from 8 mm of diameter to: 7 mm, 3.2 mm, 2.8 and 2 mm.

Characterizations

The structural study was carried out applying the optical microscope Olympus GX51 with an image analysis system LECO IA32. Longitudinal and transversal samples were included with high-density phenolic resin and prepared by mechanically polishing with 180 µm to 1200 µm SiC papers. The final polishing was carried out by 6 µm, 3 µm and 1 µm diamond paste. The metallographic etching used was a solution of (2%) Nital. The samples for EBSD studies were prepared with a specific technique developed for this material. Scanning electron microscopy (SEM) studies were conducted with a FEI Quanta 200 microscope. The interlamellar spacing (λ) measurements were carried out in the centre and the periphery of the wires. Microscopic details into the ferrite lamellae and microtexture are determined by electron backscatter diffraction (EBSD) and the OIM software of EDAX. The carbides stability and epsilon carbide precipitation possibility, was predicted through thermodynamic simulation carried out by FactSage 7.1., applying the FSteel and Misc databases. In order to verify the presence of the dynamic strain aging at low temperatures, differential thermal analysis (DTA) tests were performed using a Shimadzu DTA60 instrument. These results are correlated with those obtained on the microstructure, texture, thermal behaviour and precipitation kinetic of the IF steel.

Results and discussion

The characterization of longitudinal and transversal samples (involving all the diameters reductions) was carried out by optical microscopy (OM). The material present a fully pearlitic structure with an admissible proportion of coarse pearlite grains (< 10%). In the **Fig. 1**, the aspect of the structure in the sample with 8 mm of diameter is observed. The structure evolution with deformation under cold drawing up to 3.2 mm, 2.8 mm and 2.2 mm shows the pearlitic grains with high deformation, in coincidence with the cold drawing direction.

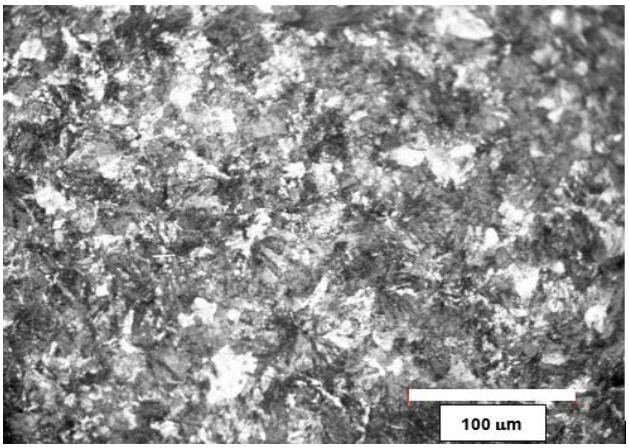

Fig.1. Fully pearlitic structure observed by optical microscopy in the wire of 8 mm of diameter before cold drawing deformation.

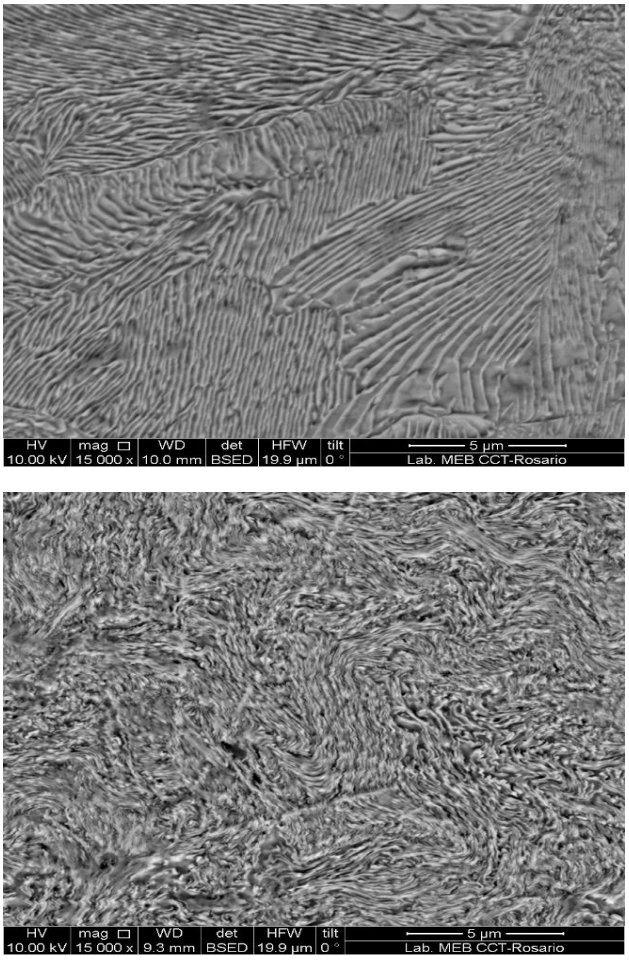

Fig. 2. Structure aspects at different wire diameters; a) ϕ = 8 mm, b) ϕ = 2 mm.

All the samples were observed by scanning electron microscopy (SEM), from 8 mm to 2 mm of diameter. The comparison between **Fig. 2 (a)** and **Fig.2 (b)**, allows to identify the curling effect on the sample cold drawn up to 2 mm of diameter. The curling effect was clearly identified in the samples with diameters: 3.2 mm, 2.8 mm and 2.2 mm. The cementite lamellae thickness also

decrease in agreement with the description mentioned in [**5**, **7**]. The thickness of cementite (Fe_3C) lamellae and the interlamellar spacing λ was determined by SEM in all the samples (diameter: 8 mm, 7 mm, 3.2 mm, 2.8 and 2 mm). A progressive refinement of the cementite lamellae was determined. In (**Table 1**), the average value of the interlamellar spacing (λ) and cementite (Fe_3C) lamellae thickness measurements, performed at ϕ=8 mm (previous to the cold drawing process) and at ϕ=2 mm after the cold drawing is presented. Krauss *et al.* [**7**] propose that the interlamellar spacing controls hardness and yield strength of the pearlitic wire. The authors confirm that the pearlite interlamellar spacing is the major microstructural parameter to control the strength of this type of steels.

Table 1. Interlamellar spacing (λ) and cementite lamellae thickness average values measured by SEM in the center and in the periphery of the wires at different cold drawn deformation levels.

Wire diameter (mm)	T_{Fe3C} centre (nm)	λ centre (nm)	T_{Fe3C} periphery (nm)	λ periphery (nm)
8	55	81	58	100
2	29	43	25	37

The cementite (Fe_3C) thickness reduction (> 40%) allows to think in the presence of a Fe_3C dissolution mechanism. The interlamellar spacing λ (nm) also present an important reduction in both zones (centre and periphery) of the wire (> 47%). The results are consistent with the information reported in the literature by different authors [**1, 2, 8**]. Ivanisenko *et al.* propose that the pearlitic steel under severe plastic deformation (SPD) also lead in the formation of non-equilibrium solid solutions, disordering or amorphization. In addition, they confirmed that during wire-drawing the cementite could be dissolved in a considerable percentage. It has also been suggested that cementite lamellae refinement may lead on their instability [**8**].

In order to increase the knowledge on the ferrite crystallographic evolution, the electron backscatter diffraction (EBSD) was applied. Nakada et al. discovered by this microscopy technique that crystal orientations of ferrite and cementite in pearlite are not completely identical and slightly rotated even in a block. They clarified that the crystal rotation cannot be attributed to high-density dislocations but it is probably due to the elastic ferrite/cementite misfit strain [9]. The interfacial structures mostly remains as elastic strain, leading in a clear crystal rotation in the pearlite. **Fig. 3 (a)**, shows the image quality map (IQ) obtained in the centre of the transversal sample (ϕ=3.2 mm) in which the curling effect is observed.

The correspondent inverse pole figure (IPF) shows that the misorientations present in the ferrite lamellaes are close to (101). It is important to mention that the IPF colour code corresponds to the direction relative to the normal direction of the observational plane. The **Fig. 3 (b)**, presents the image quality map (IQ) obtained in the longitudinal sample (ϕ = 3.2 mm). In this case, the

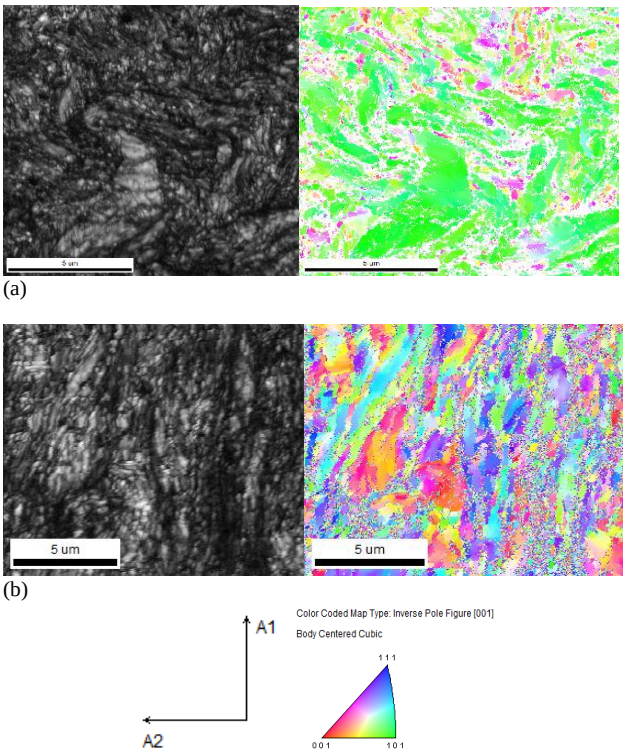

Fig. 3. Image quality maps (IQ) and inverse pole figure (IPF) obtained in the samples cold drawn up to 3.2 mm of diameter; (a) transversal sample, (b) longitudinal sample.

correspondent IPF image shows that misorientations in the ferrite are quite different respect the transversal sample. The main misorientations are associated with (111) and (001). In agreement with Ivanisenko *et al.* [**8**], the low angle misorientations are < 5º. On the contrary, the maximum of the high angle misorientations is determined at ≈ 50º. The confidence index map (CI) indicates zones not well indexed. **Fig. 4**

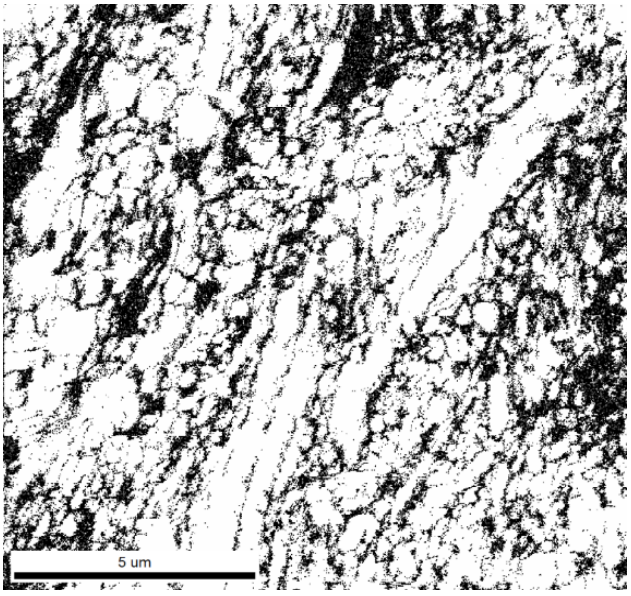

Fig. 4. Confidence index map **(**CI) showing zones not well indexed.

It is possible to think that these zones are probably associated with the carbon presence or epsilon carbides precipitates, which could be present within nano-grain boundaries. The DTA curves corroborate the epsilon carbide precipitation at low temperatures in cold drawn samples up to ϕ =2.0 mm. In addition, it is observed that the peak temperature increases with the deformation level, from T_p=168ºC (ϕ=8 mm) to T_p= 354ºC (ϕ=2.2 mm). **Fig. 5**

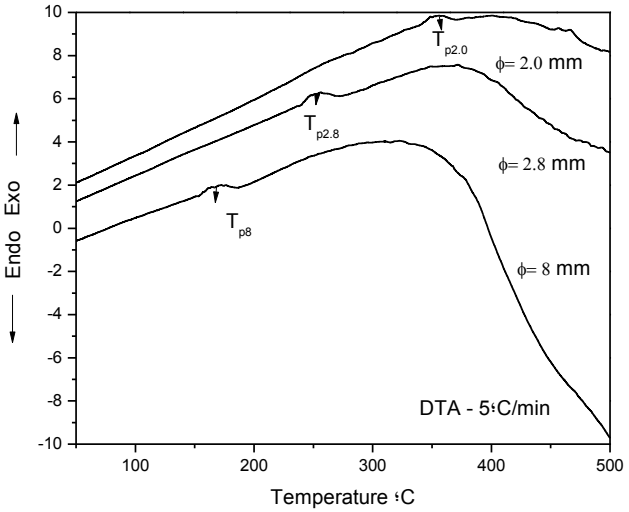

Fig. 5. DTA curves of wire samples with different deformation level.

Through thermodynamic simulation [**10**], it is possible to corroborate that the Fe_3C is the most stable iron carbide. However, ultra-high deformation could destabilized the cementite and promotes the lamellae dissolution. The ferrite over-saturation with carbon probably induces the epsilon carbide ($Fe_{2.5}C$) precipitation at low temperatures because of their nearest Gº(J) values. **Fig. 6**

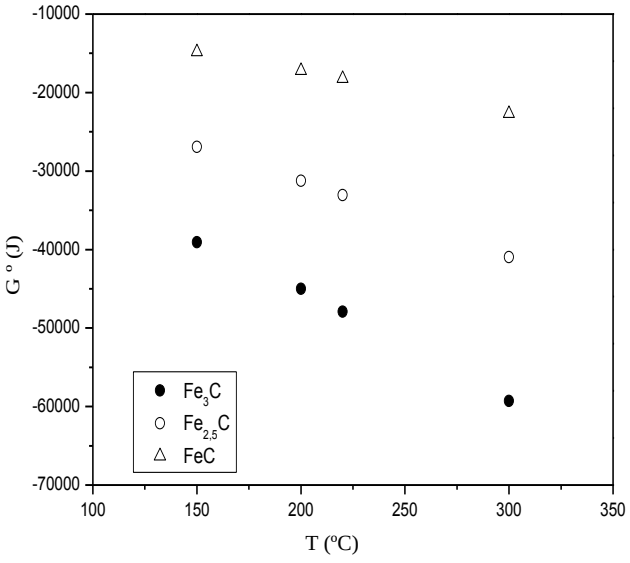

Fig. 6. Iron carbides stability in relation with temperature, predicted by thermodynamic simulation.

In agreement with Nakada *et al.* [**9**], the strength of pearlitic steel cannot be fully explained by the interlamellar spacing. The evolution of the ferrite/cementite elastic misfit strain strengthens the ferrite matrix and contributes to the extraordinary high strength of the material. Kumar *et al.* propose that the interlamellar stress at the interface can reach as high as 2000 MPa and causes the accumulation of misfit dislocation [**1**]. Ivanisenko *et al.* [**8**] confirm that for high plastic deformation, the ferrite phase is very inhomogeneous with cellular structure areas and nanostructured regions with elongated grains. The grains are separated by dense dislocation walls. The formation of nanostructure during SPD consists in three stages. The first stage corresponds to the formation of cell structure. Further increase of strain leads to an increase in the number of dislocations in the cell walls. The rearrangements and annihilation of dislocations in the cell boundaries results in high angle grain boundary formation (third stage). This information is consistent with the results obtained in the IPF and CI maps for the longitudinal sample by EBSD, see **Fig. 5** and **Fig. 6.** The authors also propose that carbon atoms segregates at grain boundaries and dislocation cores. The carbon atoms in the interstitial sites of iron matrix produce a change of lattice parameter. On this base and the evidence of the epsilon carbide precipitation (determined by DTA tests), it is possible to justify the presence of not well indexed zones visualized in the ferrite structure and the association of them with cell boundaries and nano-grains boundaries that contribute to develop high strength in the pearlitic wire, see **Fig. 6.**

Conclusion

The optical microscopy characterization of the pearlitic wire (longitudinal and transversal) samples with different deformation level (ϕ=8 mm → ϕ=2.2 mm) allows to determine that the material presents a fully pearlitic structure with admissible proportion of coarse pearlite grains (< 10%). Through scanning electron microscopy the curling effect in the samples cold drawn at 3.2, 2.8 and 2.2 mm of diameter was identified.

The cementite (Fe_3C) lamellae thickness reduction (> 40%) shows the evidence of its dissolution mechanism. The decrease of the interlamellar spacing λ (nm) also is important (> 47%) in the transversal section of the wire. Both aspects contribute to the mechanical strength increment. However, other factors are present in the structure in order to achieve the required mechanical properties.

The EBSD technique application permits to verify the ferrite structure evolution during cold drawing. The microtexture differences between the transversal and longitudinal samples are determined through the IPF maps. In addition, low angle misorientations (< 5º) and high angle misorientations (≈ 50º) are present in the ferrite. In the longitudinal samples, the IPF maps shows the presence of a ferrite structure compatible with cells and nano-grains. In agreement with Ivanisenko *et al.* this

structural characteristics generated after SPD constitute an important factor to achieve the extraordinary strength in the wire. The CI map corroborates the presence of zones not well indexed probably associated with carbon presence or epsilon carbide precipitates in the nano-grains boundaries.

The comparison of the DTA curves of the wires with different deformation levels shows that the epsilon carbide precipitation peak temperature could increase with the cold drawn deformation level up to T≈ 350ºC. The result are consistent with the structural characterization and the thermodynamic study of iron carbides, justifying the presence of strain aging mechanism and their association with the nano-grains structure.

Acknowledgements

The authors gratefully acknowledges the financial support received by the Universidad Tecnológica Nacional. The authors also thank Dr. R. Bolmaro at IFIR CONICET for helpful discussions on the curling effect and deformation mechanisms.

References

1. Kumar, P.; Gurao, N.P.; Haldar, A.; and Suwas, S.; *ISIJ International*; **2011**, 51, 4, 679. **DOI:** 10.2355/isijinternational.ISIJINT/51/4/51/4/679
2. Zelin, M.; *Act. Mat.*; **2002**, 50, 4431. **DOI:** 10.1016/S1359-6454(02)00281-1
3. Nam, W.J.; Bae, C.M.; Oh, S.J.; Kwon, S.J.; *Scripta mater*; **2000,** 42, 457. **DOI:** 10.1016/S1359-6462(99)00372-3
4. Gavriljuk, V. G.; *Scripta Materialia;* **2001**, 45, 1469. **DOI:** 10.1016/S1359-6462(01)01192-7
5. Krauss, G.; (2nd Eds.); Steels processing, structure and performance; ASM International, USA, **2005**. **ISBN:** 0871708175 (ISBN13: 9780871708175)
6. Nematollahi, G. A.; Pezold, J.; Neugebauer, J.; Raabe, D.; *Acta Materialia*, **2013**, 61, 1773. **DOI:** 10.1016/j.actamat.2012.12.001
7. Brandaleze, E.; *Procedia Mat. Scien*.; **2015**, 8, 1023. **DOI:** 10.1016/j.mspro.2015.04.164
8. Ivanisenko, Y.; Lojkowski, W.; Valiev, R.Z.; Fecht, H.J.; *Act. Mat.*, **2003**, 51, 5555. **DOI:** 10.1016/S1359-6454(03)00419-1
9. Nakada, N.; Koga, N.; Tanaka, Y.; Tsuchiyama, T.; Takaki, S.; Ueda, M.; *ISIJ International*; **2015**, 55, 9, 2036. **DOI:** 10.2355/isijinternational.ISIJINT-2015-102
10. Bale, C. W.; Bélisle, E.; Chartrand, P.; Degterov, S. A.; Eriksson G.; Gheribi, A.E.; Hack, K.; Jung, H.J.; Kang, Y.B.; Melançon, J.; Pelton, A.D.; Petersen, S.; Robelin, C.; Sangster, J.; Spencer, P.; Van Ende, M.A.; *Calphad*, **2016**, 54, 35. **DOI:** 10.1016/j.calphad.2016.05.002

